Proceedings of the European Conference Physics of Magnetism 2011 (PM'11), Poznań, June 27–July 1, 2011

Mössbauer Study of Magnetic Properties of $Fe_{80-x}Co_xZr_7Si_{13}$ ($x = 0$–30 at.%) Boron-Free Amorphous Alloys

M. Kopcewicz[a], A. Grabias[a], J. Latuch[b], J. Ferenc[b], R. Żuberek[c] and K. Nesteruk[c]

[a]Institute of Electronic Materials Technology, Wólczyńska 133, 01-919 Warszawa, Poland

[b]Faculty of Materials Science and Engineering, Warsaw University of Technology Wołoska 141, 02-507 Warszawa, Poland

[c]Institute of Physics, Polish Academy of Sciences, al. Lotników 32/46, 02-668 Warszawa, Poland

Amorphous $Fe_{80-x}Co_xZr_7Si_{13}$ ($x = 0$–30 at.%) alloys in which boron was completely replaced by silicon as a glass forming element have been prepared by melt quenching. Partial substitution of iron by cobalt caused the increase of the hyperfine field and saturation magnetization. The specialized rf-Mössbauer measurements revealed that all amorphous alloys studied are magnetically very soft. The rf-sidebands effect, related to magnetostriction, increases with the increase of Co content. In $Fe_{50}Co_{30}Zr_7Si_{13}$ sample the rf field exposure induced partial crystallization of amorphous phase that was attributed to mechanical deformations related to high frequency magnetostrictive vibrations induced by the rf field. The measurements of the hysteresis loop revealed that coercivity increases for higher Co content.

PACS: 75.50.Kj, 75.60.−d, 76.80.+y, 82.80.Ej

1. Introduction

Amorphous Fe-based alloys have been studied extensively not only from the fundamental point of view but also due to their excellent soft magnetic properties attractive for technical applications [1–3]. Recently, boron that is commonly used as a glass forming element was replaced by a cheaper element — Si [4]. Boron-free $Fe_{80}Zr_xSi_{20-x-y}Cu_y$ amorphous alloys were produced recently in the composition range of $x = 6$–10 and $y = 0, 1$ [5]. The aim of the present study is the preparation by rapid quenching and structural and magnetic characterization of amorphous $Fe_{80-x}Co_xZr_7Si_{13}$ ($x = 0$–30) boron-free alloys. In order to increase the saturation magnetization and the hyperfine field at Fe sites iron was partially substituted by cobalt [6, 7].

2. Experimental details

Amorphous $Fe_{80-x}Co_xZr_7Si_{13}$ ($x = 0$–30) alloys have been prepared in Ar by melt quenching technique. The as-quenched ribbons were 1 mm wide and about 30 μm thick. The as-quenched amorphous alloys were characterized by the Mössbauer spectroscopy, X-ray diffraction (XRD) and differential scanning calorimetry (DSC).

The DSC measurements were carried out in order to estimate the crystallization temperatures of the amorphous alloys. The heating rate of 20 K min^{-1} was applied. The XRD measurements were performed using a Cu K_α radiation. Conventional Mössbauer measurements in the transmission geometry were performed at room temperature. A conventional constant acceleration spectrometer with a ^{57}Co-in-Rh source of activity about 50 mCi was used. Soft magnetic properties of amorphous alloys have been studied by a specialized "rf-Mössbauer" technique in which the spectra were measured during exposure of the sample to the radio-frequency (rf) field of 0 to 20 Oe at 61 MHz. Coercive fields of the amorphous alloys were determined basing on the measurements of quasi-static hysteresis loops carried out by the hysteresis loop tracer [8]. The saturation magnetization was estimated from the vibrating sample magnetometer (VSM) measurements. The saturation magnetostriction constant, λ_S, was estimated from the measurements at room temperature using a strain modulated ferromagnetic resonance (SMFMR) method [9].

3. Results and discussion

Crystallization temperatures of amorphous $Fe_{80-x}Co_xZr_7Si_{13}$ alloys determined by DSC measurements are listed in Table. The DSC curves for all alloys studied ($x = 0$, 10, 20, 30) exhibit two exothermic peaks, showing that alloys crystallize in two steps. The DSC curve recorded for $x = 0$ reveals only one step at 614 °C, the second crystallization peak appears beyond the temperature range studied (50–720 °C). As can be

seen from Table all crystallization temperatures decrease with increasing Co content in the alloy.

TABLE

Onset temperatures of crystallization (T_{x1}) and of the first (T_{P1}) and second (T_{P2}) DSC peaks.

Alloy composition	T_{x1} [°C]	T_{P1} [°C]	T_{P2} [°C]
$Fe_{80}Zr_7Si_{13}$	598	614	*
$Fe_{70}Co_{10}Zr_7Si_{13}$	585	611	693
$Fe_{60}Co_{20}Zr_7Si_{13}$	513	588	679
$Fe_{50}Co_{30}Zr_7Si_{13}$	503	565	668

* The second crystallization step (T_{P2}) is expected at temperatures exceeding the temperature limit of DSC-7 calorimeter (720 °C).

The XRD patterns of all as-quenched FeCoZrSi alloys consist of a broad diffuse peak that indicate that the as--quenched alloys were amorphous. In the XRD pattern of the alloy containing 30 at.% Co a trace of the sharp peak was detected that suggests that a nanocrystalline phase of marginal volume fraction was formed during quenching, most probably at the surface of the ribbon.

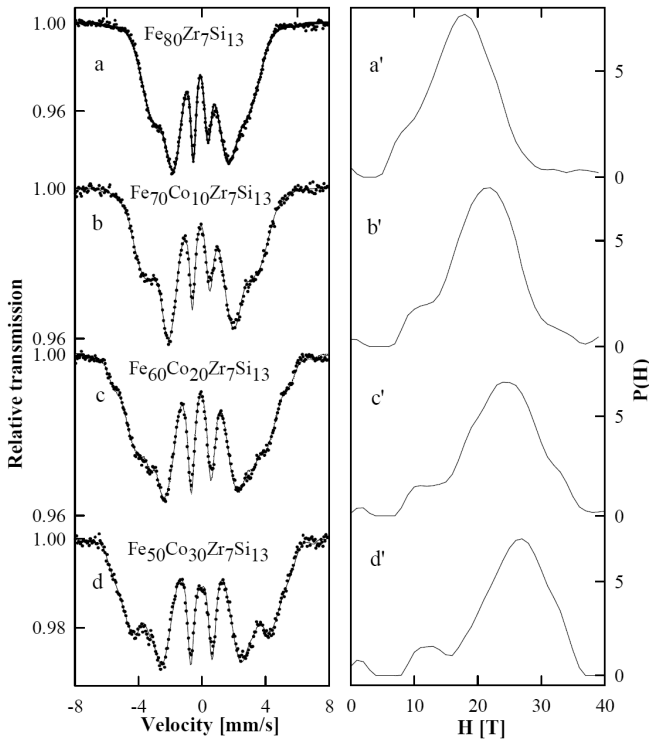

Fig. 1. Mössbauer spectra and corresponding $P(H)$ distributions for amorphous alloys (compositions indicated).

The conventional Mössbauer spectra recorded for $Fe_{80-x}Co_xZr_7Si_{13}$ alloys with $x = 0$, 10, 20 and 30 are shown in Fig. 1 together with the distributions of hyperfine fields, $P(H)$, extracted from the corresponding spectra using the NORMOS program. All spectra consist of a sextet which is broadened due to the distribution of hyperfine fields. All $P(H)$ distributions consist of a fairly symmetric main peak (Fig. 1a′–d′). For the amorphous $Fe_{80}Zr_7Si_{13}$ alloy the dominating peak at about 19 T is accompanied by a "shoulder" at about 10 T (Fig. 1a′). Partial substitution of iron by cobalt causes the increase of the average values of the hyperfine field to 21.5 T, 25.0 T, and 27.0 T for $x = 10$, 20 and 30, respectively (Fig. 1b′–d′). The increase of hyperfine fields observed for increasing Co content in amorphous FeZrSi alloys was associated with a significant increase of coercivity. The coercive fields were determined from the hysteresis loop tracer [8] under a small magnetic field applied, up to ±660 A m^{-1} (Fig. 2). The estimated coercive fields increase from 19 A m^{-1} for $Fe_{80}Zr_7Si_{13}$ alloy to 42 and 168 A m^{-1} for alloys containing 20 and 30 at.% of Co, respectively. The saturation magnetization estimated from VSM measurements varied from 119 emu g^{-1} for $Fe_{80}Zr_7Si_{13}$ alloy to 123 and 127 emu g^{-1} for Co-containing alloys with $x = 20$ and 30, respectively.

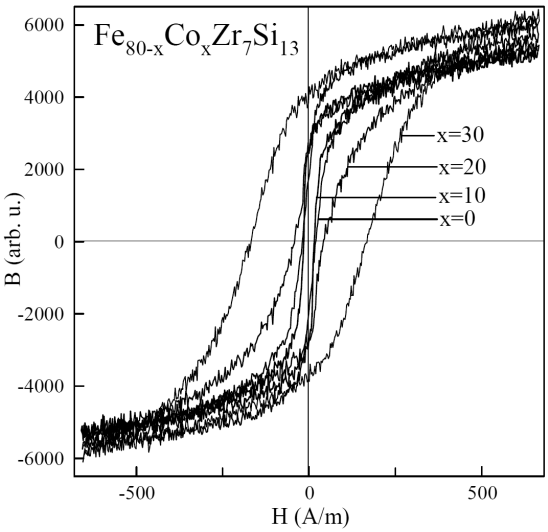

Fig. 2. Hysteresis loops recorded for amorphous $Fe_{80-x}Co_xZr_7Si_{13}$ alloys using hysteresis loop tracer.

Soft magnetic properties of amorphous $Fe_{80-x}Co_xZr_7Si_{13}$ alloys have been studied by the specialized "rf-Mössbauer" technique which combines the Mössbauer effect with the phenomena induced by an external radio-frequency magnetic field: the rf-collapse and rf-sideband effects. For a detailed discussion of the rf field induced effects see, e.g., [3, 10, 11]. The rf-Mössbauer spectra measured during exposure of the sample to the rf field of intensity ranging from 0 to 20 Oe at the frequency of about 61 MHz revealed that all alloys studied are magnetically very soft. As an example the Mössbauer spectra recorded for $Fe_{80}Zr_7Si_{13}$ and $Fe_{50}Co_{30}Zr_7Si_{13}$ amorphous alloys are shown in Fig. 3. In the case of $Fe_{80}Zr_7Si_{13}$ alloy the rf-collapse of magnetic hyperfine structure (mhfs) to a nonmagnetic

pattern due to fast magnetization reversal induced by the rf field whose intensity exceeds the local anisotropy field, is observed at a fairly small intensity of 6 Oe (Fig. 3b). The central doublet is accompanied by the rf-sidebands that are directly related to magnetostriction of the alloy [10]. The absorption lines of the rf-collapsed doublet narrow with the increase of the rf field intensity and stabilize at about 10 Oe (Fig. 3c). Thus the complete rf-collapse of mhfs is observed at 10 and 20 Oe (Fig. 3c–d). The shapes of the spectra recorded in the absence of rf field before and after exposure to the rf field are identical (Fig. 3a and Fig. 3e) suggesting that the rf field exposure did not induce permanent changes in the sample. The rf-Mössbauer spectra recorded for $Fe_{50}Co_{30}Zr_7Si_{13}$ alloy were significantly different. At small rf field (6 Oe) the spectrum is only marginally affected by the rf field (Fig. 3b′). At larger intensity of the rf field (10 Oe, Fig. 3c′) a broadened rf collapsed doublet appears, accompanied by the resolved magnetic spectral component. At 20 Oe the rf-Mössbauer spectrum is complex (Fig. 3d′). It contains a central rf-collapsed doublet accompanied by well defined rf-sidebands. Much larger intensities of sidebands observed for $Fe_{50}Co_{30}Zr_7Si_{13}$ alloy (Fig. 3d′) than for $Fe_{80}Zr_7Si_{13}$ alloy (Fig. 3d) strongly suggest that magnetostriction constant is significantly larger for Co-containing alloy than for Co-free alloy. In addition to the rf-collapsed doublet and rf-sidebands the magnetic hyperfine structure is observed in Fig. 3d′. This spectral component was fitted with a sextet that originates from the nanocrystalline FeCo phase, which is magnetically much harder than the amorphous phase. The Mössbauer spectrum recorded after rf field exposure (Fig. 3e′) is significantly different as compared with that recorded before rf field exposure (Fig. 3a′). The spectrum recorded before rf field exposure does not reveal crystalline spectral component and consists of a broadened sextet. The spectrum recorded after rf field exposure contains, in addition to the broadened sextet originating from the amorphous phase, a sextet related to the nanocrystalline FeCo phase with the large magnetic hyperfine field of about 36 T. This sextet contributes to about 20% of the total spectral area.

In order to suggest the origin of the rf induced crystallization of Co-containing alloy and to verify whether the rf-crystallization effect is of thermal or non-thermal origin it is necessary to estimate the temperature of the sample during exposure to the rf field. This temperature can be estimated assuming that the entire center shift of the spectrum recorded during the rf field exposure is caused by the heating effect and can be related to the second order Doppler (SOD) shift [12]. The SOD shift for a given alloy was estimated from the Mössbauer measurements performed for $Fe_{80}Zr_7Si_{13}$ and $Fe_{50}Co_{30}Zr_7Si_{13}$ alloys at well defined temperatures. The temperature of the sample during rf field exposure was estimated by comparing the change of the center shift of the rf-Mössbauer spectrum with those recorded for the same sample at room

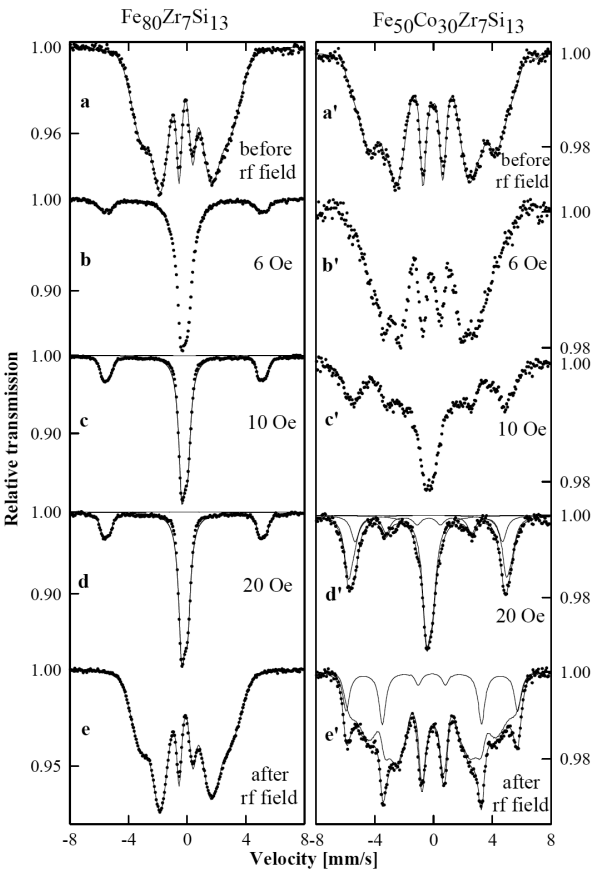

Fig. 3. Mössbauer spectra recorded for amorphous $Fe_{80}Zr_7Si_{13}$ (b–d)) and $Fe_{50}Co_{30}Zr_7Si_{13}$ (b′–d′) alloys during rf exposure to the increasing rf field intensity and the spectra recorded in the absence of the rf field: (a) and (a′) before and (e) and (e′) after rf field exposure.

temperature in the absence of the rf field and by dividing this difference by the relevant SOD factor. The temperatures estimated were about 120 °C, 187 °C, 270 °C and 295 °C for the alloys with $x = 0$, 10, 20 and 30, respectively. As can be seen, the temperatures of the samples of the alloys studied were much lower than the crystallization temperatures (Table). Therefore, the origin of the rf field induced crystallization effect as resulting from heating the sample by the rf field is excluded as a major mechanism that causes crystallization.

Crystallization may originate from non-thermal effect related to mechanical deformations [13]. It is concluded that the rf field induced crystallization is related to magnetostriction. The magnetostriction constant, λ_S, estimated from SMFMR measurements, varied from 11×10^{-6} and 16×10^{-6} for $x = 0$ and $x = 10$ alloys, respectively, to 24.1×10^{-6} and 24.5×10^{-6} for $x = 20$ and $x = 30$, respectively. The rf field induced crystallization, particularly pronounced in $Fe_{50}Co_{30}Zr_7Si_{13}$ alloy that reveals significantly larger λ_S than that observed for $Fe_{80}Zr_7Si_{13}$ alloy, was attributed to mechanical deformations induced in the sample via magne-

tostriction. The rf field forced enhanced vibrations of atoms as a result of which the amorphous structure was destabilized and partly crystallized (see also [12]). These vibrations cause the formation of rf-sidebands in the rf-Mössbauer spectra. The rf-sidebands observed in Fig. 3d′ for $Fe_{50}Co_{30}Zr_7Si_{13}$ alloy are significantly larger than these observed in Fig. 3c, d for $Fe_{80}Zr_7Si_{13}$ alloy that was attributed to considerably larger magnetostriction of Co-containing alloy.

Acknowledgments

The financial support from the grant No. N 507 278636 from the Ministry of Science and Higher Education (Poland) is gratefully acknowledged.

References

[1] M.E. McHenry, W.A. Willard, D.E. Laughlin, *Prog. Mater. Sci.* **44**, 292 (1999).

[2] A. Makino, A. Inoue, T. Matsumoto, *Mater. Trans. JIM* **36**, 924 (1995).

[3] M. Kopcewicz, in: *Handbook of Advaced Magnetic Materials*, Vol. II, Eds. D.J. Sellmyer, Y. Liu, D. Shindo, Tsingua University Press/Springer, Beijing 2006, p. 151.

[4] J. Long, D.E. Laughlin, M.E. McHenry, *J. Appl. Phys.* **103**, 07E708 (2008).

[5] M. Kopcewicz, A. Grabias, J. Latuch, M. Kowalczyk, *Mater. Chem. Phys.* **126**, 669 (2011).

[6] J.S. Blazquez, A. Conde, J.M. Greneche, *Appl. Phys. Lett.* **81**, 1612 (2002).

[7] K. Suzuki, J.W. Cochrane, J.M. Cadogan, X.Y. Xiong, K. Ono, *J. Appl. Phys.* **91**, 8417 (2002).

[8] T. Kulik, H.T. Savage, A. Hernando, *J. Appl. Phys.* **73**, 6855 (1993).

[9] R. Żuberek, K. Fronc, A. Szewczyk, H. Szymczak, *J. Magn. Magn. Mater.* **260**, 386 (2003).

[10] M. Kopcewicz, *Struct. Chem.* **2**, 313 (1991).

[11] M. Kopcewicz, *J. Alloys Comp.* **382**, 165 (2004).

[12] M. Kopcewicz, *J. Appl. Phys.* **103**, 07E717 (2008).

[13] M.L. Trudeau, R. Schulz, D. Dassaults, A. Van Neste, *Phys. Rev. Lett.* **64**, 99 (1990).